Thin film morphology and crystal structure of the poly(*p*-phenylene terephthalamide)/sulphuric acid system

E. J. Roche, S. R. Allen, V. Gabara and B. Cox
E. I. du Pont de Nemours and Co., Central Research and Development and Fibers Departments, Experimental Station, PO Box 80356, Wilmington, DE 19880-0356, USA
(Received 13 October 1988; revised 20 January 1989; accepted 24 January 1989)

The morphology and crystal structure of poly(*p*-phenylene terephthalamide) (PPTA) thin films shear-cast from concentrated sulphuric acid solutions have been investigated, with emphasis on the effects of molecular weight, quench rate and coagulant. The films exhibit the banded optical texture typical of the relaxation patterns of liquid crystal polymers, except in the case of very thin films. On a finer scale, row-nucleated structures are observed for low quench rates and fibrillar structures for higher rates or direct coagulation experiments. The periodicity of the row-nucleated structure is related to the polymer chain length. In the case of delayed coagulation, a crystallosolvate structure is obtained which, upon subsequent crystallization, collapses into either of the two PPTA polymorphs depending on the extraction conditions. A polymorphic transformation scheme is proposed accordingly. The results are discussed in relation to fibre properties.

(Keywords: Kevlar; crystallosolvate; crystalline polymorphism; electron microscopy; poly(*p*-phenylene terephthalamide) film; optical texture)

INTRODUCTION

A considerable body of literature has accumulated concerning the morphology of liquid crystal polymers, most of it centred about the banded optical texture so typical of these systems. Poly(*p*-phenylene terephthalamide) (PPTA) is the best known of these polymers, in the form of the high performance Kevlar® fibres[1,2]. Some of the outstanding structural features of these fibres were initially described by Ballou[3] and Dobb *et al.*[4] More recently, Horio *et al.*[5] reexamined how the fibre optical texture relates to the banded texture of PPTA films. Quite in contrast, the associated crystalline morphologies have been found to be rather similar to those of ordinary flexible polymers. Takahashi *et al.*[6], for example, showed that strain-induced crystallization of PPTA from sulphuric acid solution resulted in row-nucleated lamellar morphologies. Lamellar morphologies were also encountered in spherulitic structures of the polymer obtained either from slow coagulation of moderately concentrated sulphuric acid solutions[6,7], or directly from the polymerization mixture[8]. In parallel to these studies, PPTA crystalline polymorphism has been described through the works of Northolt[9], who described the crystal structure (PPTA I) encountered in the fibres, and of Haraguchi *et al.*[10] who identified a second polymorph, PPTA II, in films coagulated in water. In addition, Arpin *et al.*[11] and Iovleva and Papkov[12] demonstrated the existence of a PPTA/H_2SO_4 complex for which Gardner *et al.*[13] later proposed a partial phase diagram. Further investigations by Xu *et al.*[14] indicated that a water complex could form upon displacement of the sulphuric acid by water.

This short review of the literature illustrates how previous studies have focused on either the optical texture of PPTA or, on a finer scale, on its lamellar morphologies slowly grown from diluted solutions. Little attention has been devoted to other factors greatly affecting the morphology, such as temperature and coagulation rate. The present work is a systematic investigation of the morphology and crystal structure of PPTA thin films with emphasis on those parameters which are very relevant to the fibre spinning process. The effects of molecular weight, quench rate and coagulant are described in light of earlier literature data. The relationship between different levels of morphology is examined and a mechanism for the crystalline polymorphic transformations is proposed. Finally, the results are discussed in relation to fibre properties.

EXPERIMENTAL

Materials

Because of the great moisture sensitivity of concentrated PPTA solutions in sulphuric acid, most experiments were conducted in a dry box under nitrogen atmosphere. For direct quenching in water, the water bath was isolated from the atmosphere of the box by an oil layer. The PPTA solutions were prepared by dissolving polymer with inherent viscosity ranging from 0.1 to 10.0 dl/g (measured in 96% H_2SO_4) in 100% sulphuric acid at 80°C to a concentration of about 20 wt%. Film casting was performed on a hot plate whose temperature was generally adjusted to about 80°C. More precisely, a crumb of the solidified PPTA/H_2SO_4 paste was deposited on a glass slide, itself on the hot plate. The progressive re-melting of the crumb was monitored via the corresponding colour change. The molten droplet was quickly sheared using a second glass slide or a razor blade. The sheared film, now having a silvery colour, was then either immediately plunged (with its supporting slide) into a quench bath, or let to relax for a few seconds before quenching. The shortest time attained between shearing and quenching was of the order of 0.3 s. Quench

0032-3861/89/101776-09$03.00

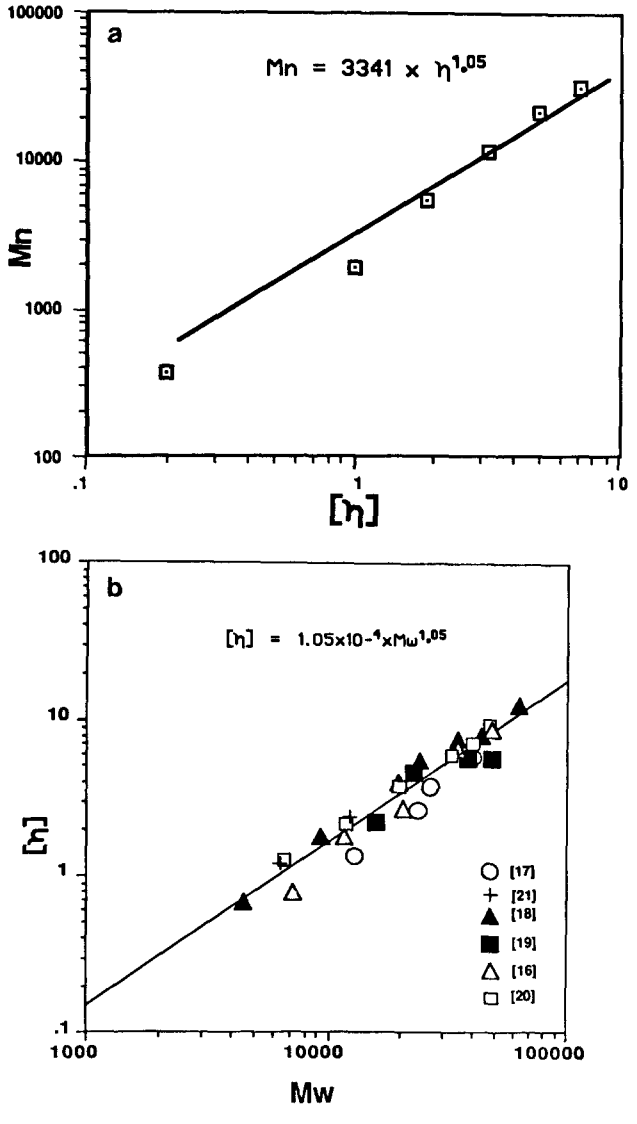

Figure 1 (a) Empirical fit of g.p.c.-determined M_n to the inherent viscosity data. (b) Comparison of present g.p.c. calibration to earlier literature data

rates were experimentally estimated as follows: a bare thermocouple was plunged into the quench bath and the corresponding rate calculated from the digitized temperature/time profiles. A similar method has recently been described[15]. Quench rates in the range of 100 to 500° s^{-1} could be achieved by varying the bath temperature from 25° to −70°C. Quench rate for an air-cooled slide was estimated at about 10° s^{-1}.

Methanol and water with 95% acetic acid and 75% formic acid were used for concomitant quench and coagulation, at room temperature. Reagent grade methylene chloride (water content <0.03%), or Freon® TF, were used for pure quench experiments, with temperatures adjusted in the range −70° to 25°C. When using the non-coagulating media the films retained their silvery colour, but turned bright yellow otherwise. For optical microscopy of the solvated structure, the films were sealed with an epoxy resin between slide and coverslip in the dry box. The films were eventually washed with water or methanol for further characterization.

Molecular weights were estimated from viscosity data using the empirical equation:

$$M_n = 3341[\eta]^{1.05}$$

This equation was obtained by fitting g.p.c. data[16] as illustrated in *Figure 1a*. *Figure 1b* further illustrates the good agreement between this calibration and earlier literature data[17–21].

Instrumentation

A Jeol 2000EX electron microscope was used, operated at 200 kV. Phase (defocus) contrast and diffraction contrast imaging modes were most effective in imaging the structure. Electron diffraction information was generally recorded, in proper register, on the same negative as the image. For small angle scattering, camera lengths in the range 20 to 80 m were used, calibrated with a 2160 lines/mm grating replica (Polaron). Selected areas in this case were about 40 μm in diameter.

A Zeiss Axioplan polarizing microscope was used for light microscopy observations. X-ray diffractometer traces were obtained with a Philips 2θ diffractometer operated in the symmetrical transmission mode. The diffractometer was mounted on a Philips 2100 generator operated at 40 kV and 40 mA. Slits of 1° were used.

RESULTS

Optical texture

Figure 2 shows polarized light micrographs (crossed-polars) of films sheared and quenched in a non-coagulating medium (room temperature methylene chloride), then sealed off from moisture. For the experiment illustrated in *Figure 2a*, some time (about 100 s) was allowed for relaxation. A hedritic crystallization was observed, with the hedrite branches growing in directions mostly perpendicular to the shear direction

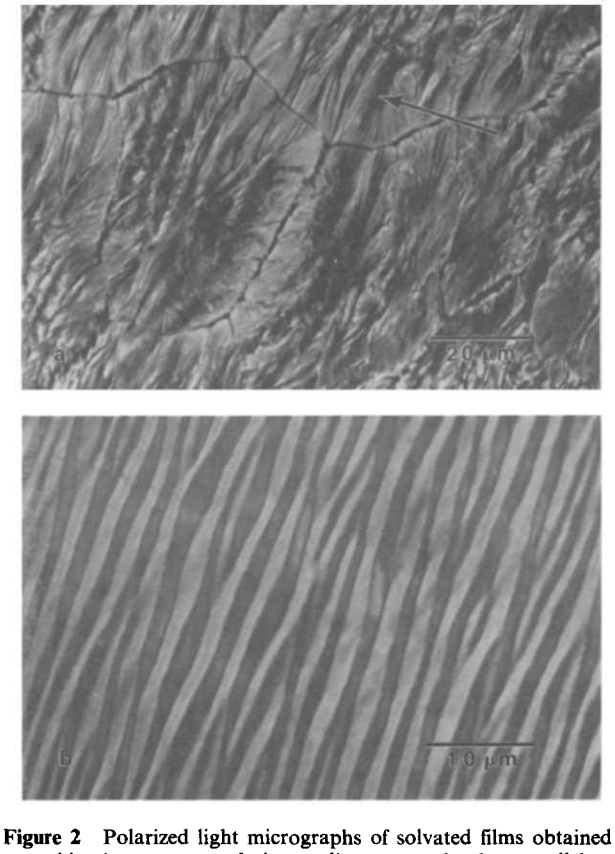

Figure 2 Polarized light micrographs of solvated films obtained by quenching in a non-coagulating medium; crossed polars parallel to the micrographs' edges. The arrow in (a) indicates the shear direction

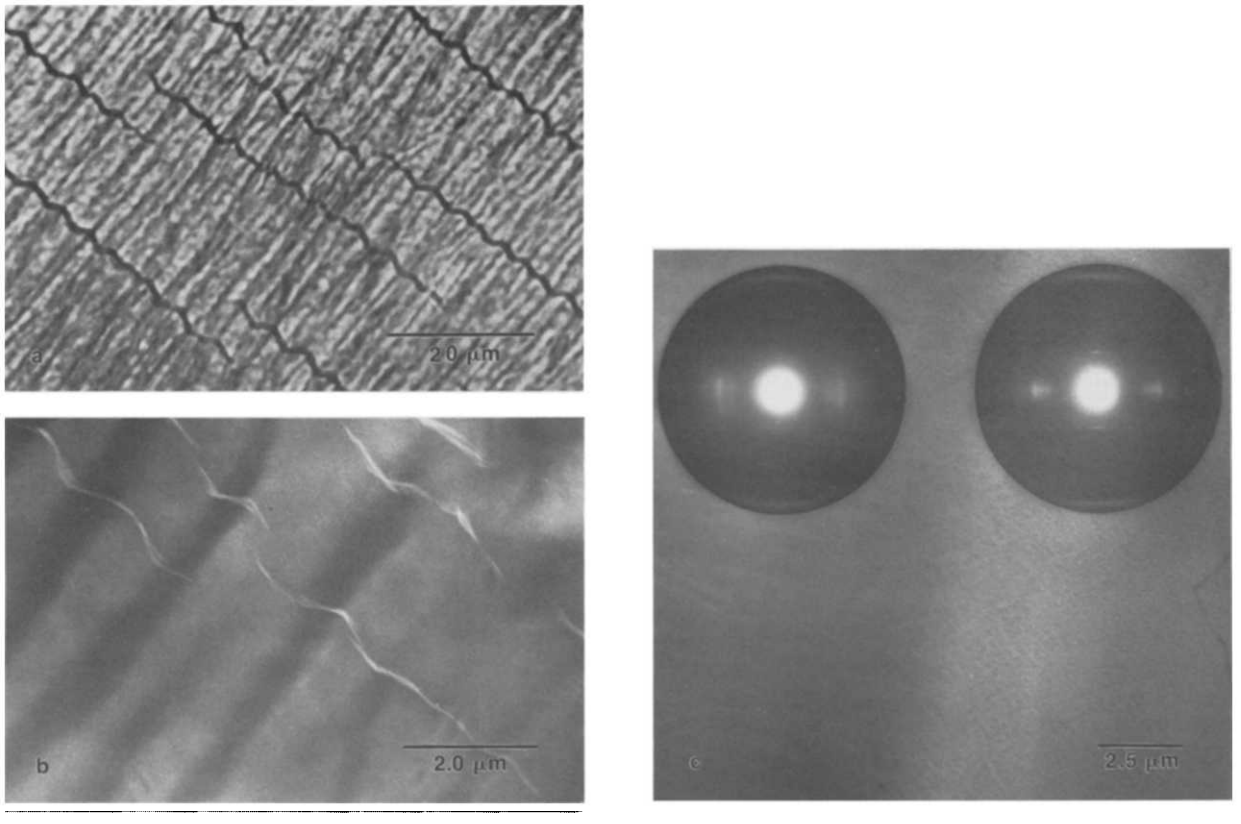

Figure 3 Compared morphologies of solvated films before and after coagulation. (a) Polarized light micrograph (crossed polars parallel to the micrographs' edges) of solvated structure; shear direction is parallel to the zig-zagging cracks. (b) Darkfield electron micrograph of thin region of same film as in (a) after water washing and drying. (c) Electron micrograph and corresponding electron diffraction patterns of film of varying thickness showing the disorientation associated with pleating. Shear direction is vertical; electron diffraction is in proper register with the image

(arrow). The hedrite boundaries are clearly visible as dark contours. Dark contrast within the hedrites corresponds to regions where the average molecular orientation is parallel to an extinction direction. This morphology corresponds to the crystallization of the PPTA/H_2SO_4 solvate, whose existence has been known for some time[12,13]. When little relaxation time, typically a few seconds only, was allowed, the classic banded texture was observed, as illustrated in *Figure 2b*. The reason for the banded contrast has been well documented for this and other liquid crystalline polymer systems[5,22,23]. It corresponds to a periodic change of the average molecular chain orientation. Some care must be exerted, however, in measuring the periodicity of the structure for the most highly oriented systems, exemplified by the case of Kevlar® fibres[5,24]. The true film periodicity is best measured from images like the one in *Figure 2b* where the shear direction makes a small angle with one of the polars. The period is here of about 2 μm, but is generally dependent on both the shear rate and the time allowed for relaxation. Attempts to prevent formation of the banded structure by going to the highest possible apparent quench rates, about 500° s^{-1}, were not successful for films of the usual 5 to 10 μm thickness selected for optical microscopy. Very thin films, however, (100–200 nm), were exceptions. This is consistent with the recent results of Chen *et al.*[22]. Relaxation is, in this case, prevented by dominant surface interaction or a more efficient quench.

Upon washing of the quenched films, the progressive exchange of sulphuric acid for water could be followed by observing the film colour change. The exchange rate was strongly dependent upon the water temperature, i.e. the slowest for the lowest temperature. Tremendous shrinkage took place upon subsequent drying, essentially in the direction perpendicular to shear. The film morphology did not change, however, and was still characterized by the banded texture. *Figure 3a* shows a polarized light micrograph of a solvated film where a well delineated system of cracks nicely defines the average molecular director orientation. After washing and drying, the film, now observed by darkfield TEM (*Figure 3b*), exhibits the same typical cracks and corresponding periodic banding. Light microscopy observation of a film undergoing coagulation showed that the period is little changed by the washing/drying operation, a confirmation that only the lateral packing of the PPTA molecules is involved at that time. Diffraction information is provided in *Figure 3c* for a film of varying thickness. In the thicker part (left), banding is present and the pattern indicates some deorientation (arcing). In the edge region (right), no banding is seen and the orientation is much higher.

Figure 4a illustrates the case of concomitant quench and coagulation. The films were coagulated in room temperature acetic acid. A substructure defining a herringbone pattern is visible within the bands. Such a feature originates from the coagulation of the polymer into ribbons, after initial relaxation into a banded texture. A detailed view of similar zig-zagging ribbons is shown in the electron micrograph in *Figure 4b* revealing its fibrillar nature. The zig-zag period is shorter in this case because the structure is observed in a thinner part of the film. At higher resolution, such images indicate that the molecular bending itself is always rather smooth.

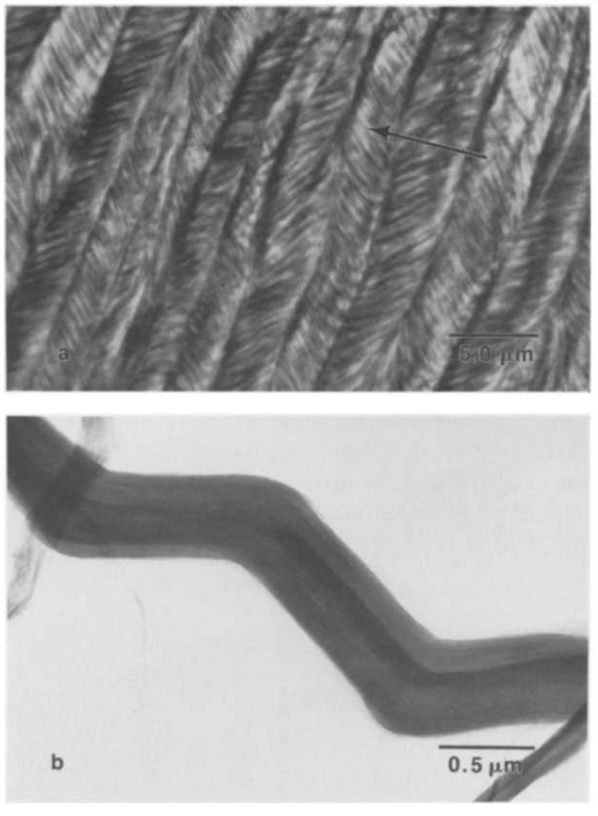

Figure 4 Morphology obtained for concomitant quench and coagulation (acetic acid bath). (a) Polarized light micrograph (crossed polars parallel to micrographs' edges). Arrow indicates shear direction. (b) Corresponding electron micrograph showing the fibrillar nature of the zig-zagging ribbons

For aqueous coagulation, two types of experiments were conducted. Firstly, the solutions were sheared and quenched/coagulated under ambient conditions. In this case, light microscopy examination revealed the presence of large crystalline structures, presumably due to humidity-induced nucleation, oriented according to the shear direction (*Figure 5a*). They are the 'rhomboids' previously described by Iovleva and Papkov[12], indicative of the crystallization of the PPTA/H_2SO_4 solvate. A high resolution micrograph (*Figure 5b*) shows their polycrystalline nature and distorted shape. The latter reflects the continuously changing orientation of the film molecular director due to shear relaxation. Secondly, the same experiment was performed in a dry atmosphere (dry box) in an attempt to prevent spurious nucleation. No rhomboidal structures were detected. In both cases, the banded texture was present in all but the thinnest films.

Fine structure

When thermal quench preceded coagulation, i.e. when the phase change path went through the crystallosolvate state, the sheared films frequently exhibited row-nucleated morphologies. This is illustrated in the electron micrographs of coagulated and dried films shown in *Figure 6*. For low quench rates (about $10° s^{-1}$), the hedrites (*Figure 6a*, also shown at lower magnification in *Figure 2a*) appear to consist of very long lamellae-like structures fanning out from the nucleus in directions roughly perpendicular to the shear direction. The 'lamellae' are about 30 nm thick and are connected by fibrillar bridges in a way quite reminiscent of the morphology of stressed PE films for example[25]. Remarkably, the long period, of the order of 120 nm, corresponds to the approximate chain length of the polymer in this case. This will be further discussed below.

The hedrite boundaries are polymer depleted regions where some interpenetration of the lamellae is observed. *Figure 6b* shows an enlarged micrograph together with the relevant electron diffraction information. The crystal structure is there PPTA II. The speckled contrast in darkfield images, as shown in *Figure 6c*, was noticed by Takahashi *et al.*[6] and interpreted as indicative of lattice distortions. More exactly, this is evidence that each lamella is polycrystalline rather than monocrystalline. The row-nucleated morphology was much less apparent for faster quench rates. *Figure 7a, b* shows morphologies obtained for a rate of about $100° s^{-1}$. The 'lamellar' overgrowth is far less developed and less voiding is apparent. The basic morphology resembles that of a 'string of pearls'. For even higher quench rates, i.e. about $500° s^{-1}$, quite fibrillar morphologies could be observed in the thinner parts of the films (*Figure 7c*).

When coagulation competed successfully with quench (water, methanol, or acid baths), no evidence for row nucleation could be detected. Fibrillar morphologies were observed instead in all cases. This is illustrated in *Figure 8a–c* for, respectively, water, methanol and acetic acid baths. The corresponding electron diffraction data indicate a PPTA I crystal structure. The splitting of the equatorial arcs in the diffraction pattern of *Figure 8a* reflects the wavery fibrillar texture of the film, again the result of shear relaxation.

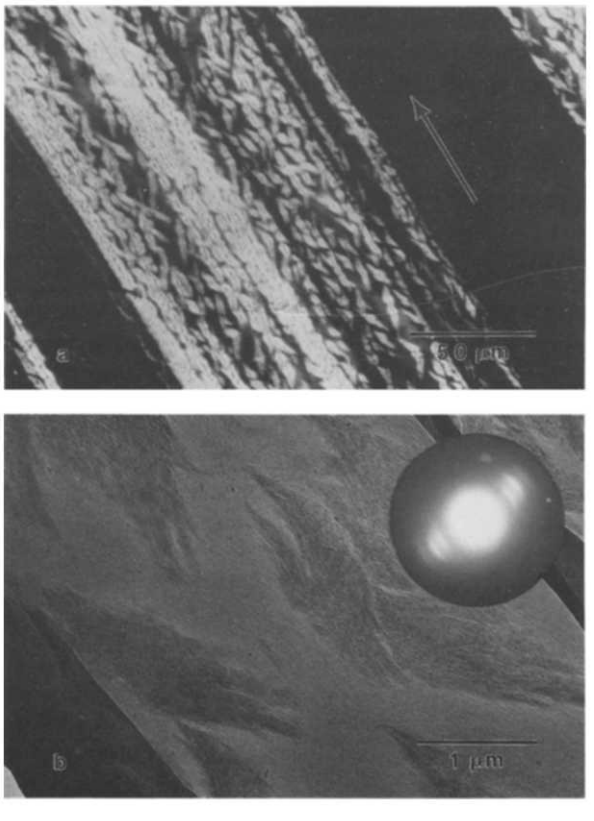

Figure 5 Rhomboid crystallosolvate structures obtained with water quench under ambient conditions. The arrow in (a) indicates shear direction. (a) Polarized light micrograph (crossed polars parallel to the micrograph's edges). (b) Corresponding electron micrograph; electron diffraction pattern was obtained from rhomboid at centre

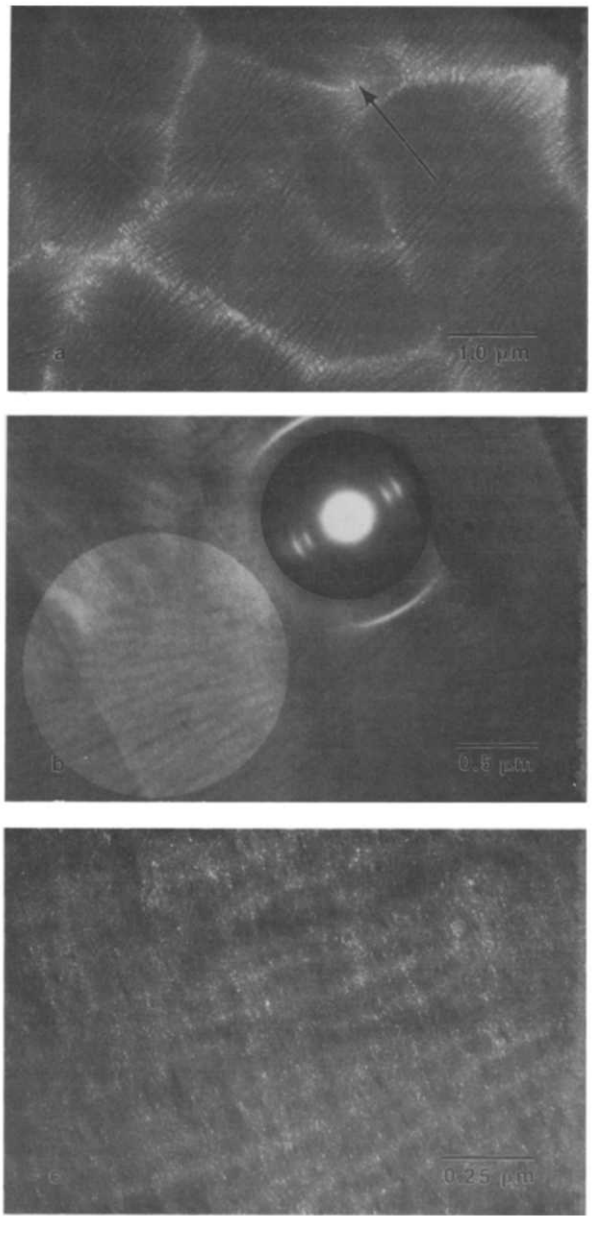

Figure 6 Electron micrographs of hedritic structure in crystallosolvate (like that shown in *Figure 2a*) after water coagulation and drying. The arrow in (a) indicates shear direction. (a) Low magnification micrograph showing boundary regions. (b) Enlarged view of (a) with electron diffraction information (from light circular area). (c) Corresponding equatorial darkfield

The findings of Haraguchi *et al.*[10] concerning the crystal structure of the coagulated films were partly confirmed in the present experiments. Namely, the polymorph type was determined by the choice of coagulant. Typically, for non-aqueous coagulants, methanol or acetic acid for example, PPTA I was obtained. For water coagulation experiments, the PPTA II structure was observed in the rhomboids of the ambient coagulation experiments (*Figure 5b*), in agreement with Haraguchi's observations. However, PPTA I was always obtained for direct coagulation (dry box experiments).

For structures with a well developed row-nucleated morphology, the electron diffraction patterns generally exhibited stronger (010) or (110) reflections (depending on the crystal structure) than (200) reflections, in agreement with earlier observations of Takahashi *et al.*[6]. Consideration of the electron diffraction geometry indicates that the (010) or (110) planes are approximately parallel to the beam, i.e. perpendicular to the film plane. The 'lamellae' grow in the plane of the film, therefore along a direction orthogonal to these planes. Such a direction is most likely [010], i.e. the hydrogen bonding direction[9,10]. This preferential orientation was not maintained in thicker films (10–50 mm thick) with banded morphology. Orientation in this case was obtained from X-ray experiments. In the diffraction experiment, the beam was perpendicular to the plane of the film, i.e. perpendicular to the plane of the 'zig-zag' pattern. A typical diffractogram is presented in *Figure 9*. A very strong (200) peak is noticed this time, indicating that hydrogen bonding is approximately perpendicular to the plane of the zig-zag, i.e. along the film thickness direction. This finding is in agreement with the original results of Haraguchi *et al.*[20] on similar films and the subsequent

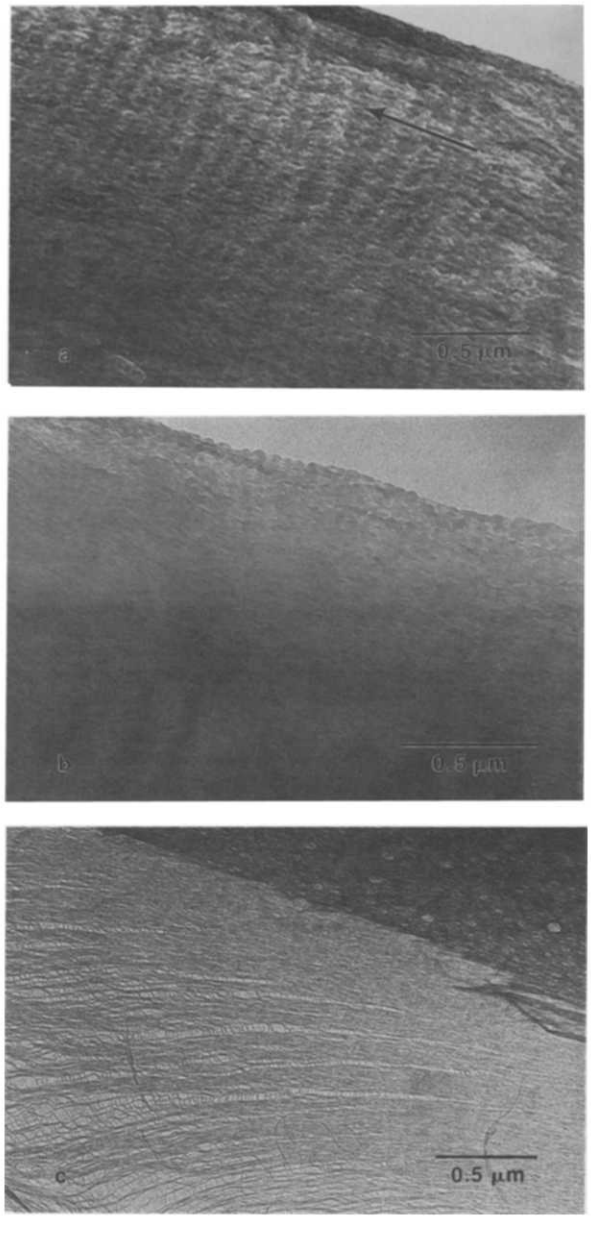

Figure 7 Electron micrograph of a methylene-chloride-quenched film after water coagulation showing the effect of quench rate on the morphology. (a), (b) 100° s^{-1} quench rate; (c) 500° s^{-1} quench rate

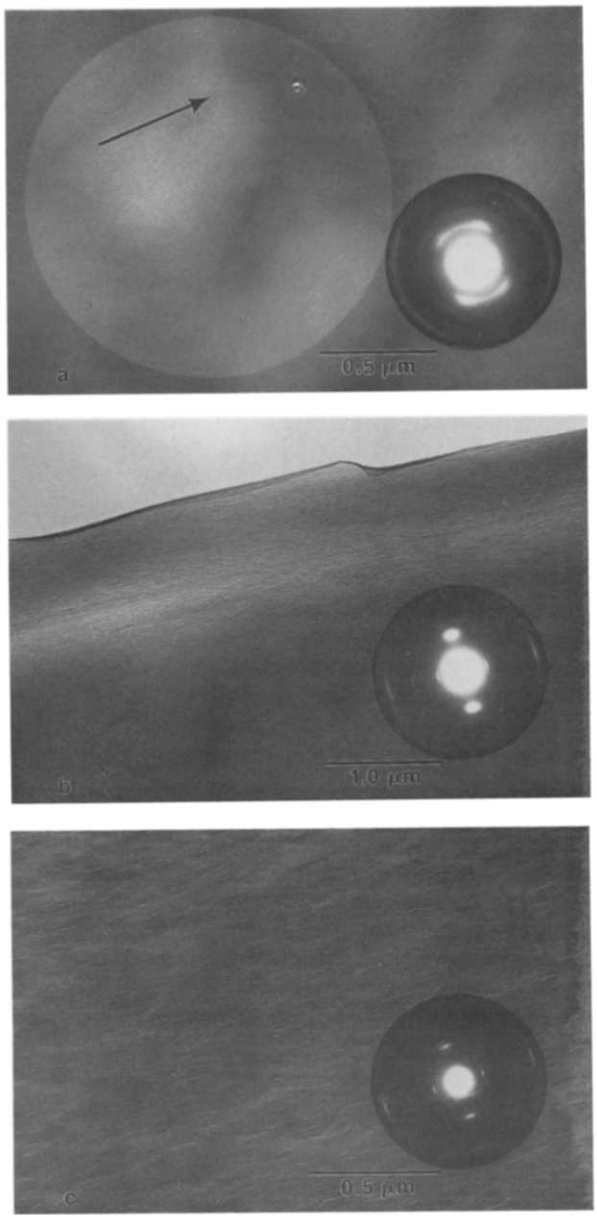

Figure 8 Fibrillar morphologies obtained with coagulating quench baths and corresponding electron diffraction data. The arrow in (a) indicates the shear direction. (a) Water; (b) methanol; (c) acetic acid

spectroscopic analysis of Shen *et al.*[27]. It is also consistent with the fibre's radial hydrogen bonding and associated pleated structure[4,5].

Thin films coagulated in acetic acid (and sometimes water) presented more peculiar orientation effects. In regions of uniform, dense, fibrillar texture, a very strong preferential orientation of the structure was indicated by the absence of the (200) reflection from the electron diffraction pattern (*Figure 8c*). Similar effects were observed in pleated ribbons like those shown in *Figure 4b*. This orientation is different from that of the row-nucleated structure. Actually, the electron diffraction data indicated a (110) spacing of 0.450 nm instead of the expected 0.438. Because the Northolt structure could be clearly identified in X-ray patterns of thicker films, it appears that specific film–substrate (glass) interactions occurred in this case. Slower coagulation resulted in enhanced features (*Figure 10a*). The morphology appears to consist of elongated structures laterally stacked together at an oblique angle to the plane of the film as schematized in *Figure 10b*. The out-of-plane lateral growth direction ((010) direction) would explain the absence of the (200) reflection in the electron diffraction pattern for normal incidence observation. The (200) reflection could not be obtained through film tilting experiments, however.

Molecular weight effects

The morphologies obtained for the various polymer molecular weights were identical in nature but with quite different values of the long period. This is exemplified by the micrographs in *Figure 11a, b* corresponding to polymer inherent viscosities of respectively 6.0 and 2.3 dl/g (for the latter polymer, the quench temperature was lowered from 25° to about −30°C to compensate

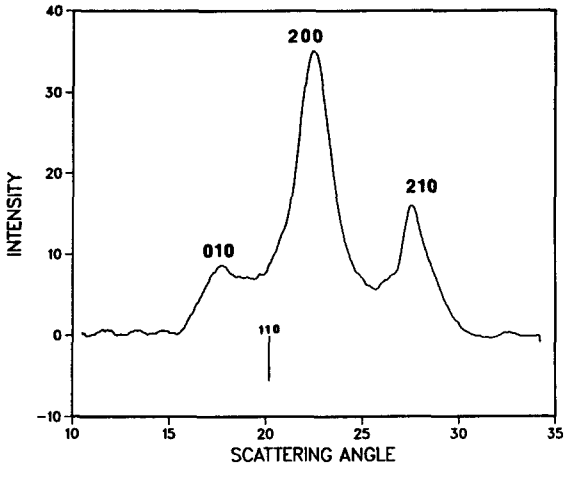

Figure 9 Equatorial X-ray diffractometer trace of a film (methylene chloride quench) with banded texture at normal incidence

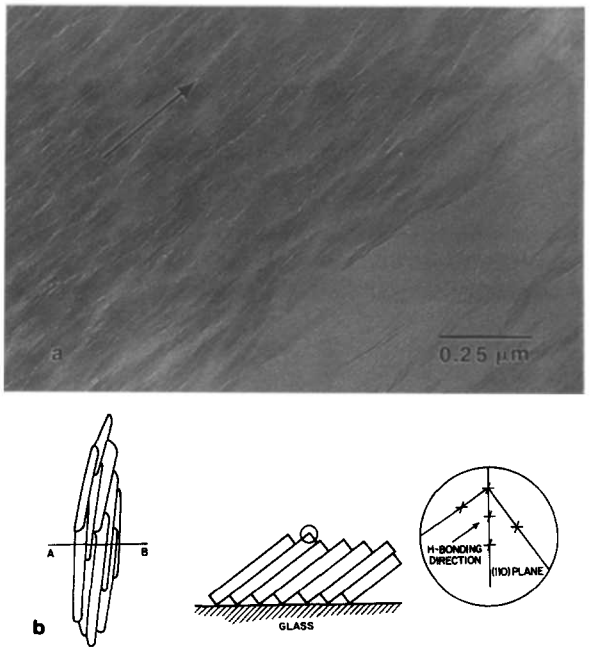

Figure 10 Preferential orientation effects with acetic acid coagulation. (a) Electron micrograph; arrow indicates shear direction. (b) Sketch of the lateral oblique stacking of the elongated structures. Left: top view (shear direction vertical); centre: cross-section along A–B. Right: enlargement of circled region in centre showing crystalline orientation

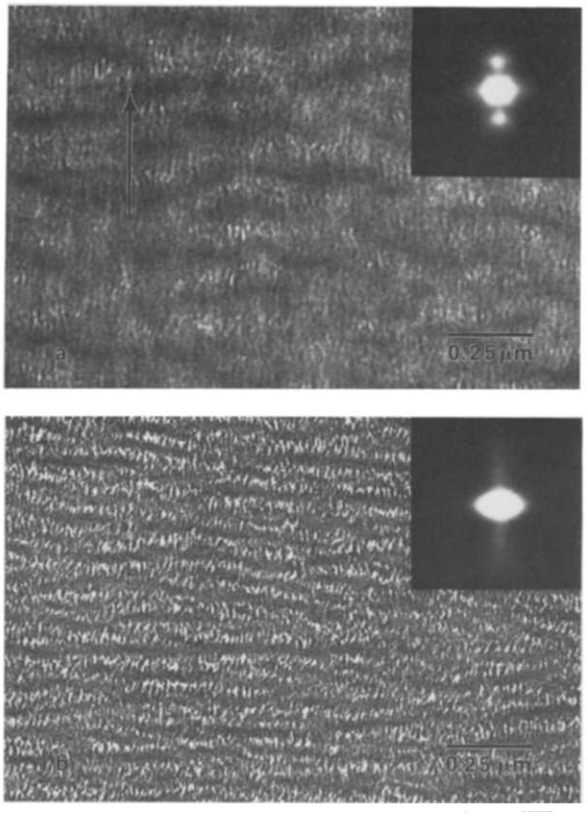

Figure 11 Electron micrographs showing the effect of molecular weight on the row-nucleated structure, and corresponding small angle electron diffraction data (insets). (a) 6.0 dl/g inherent viscosity; (b) 2.3 dl/g inherent viscosity

for the decreased viscosity of the solutions, fluid at room temperature). Both the 'lamellar' thickness and long period vary greatly, from, respectively, 10 to 30 nm and 60 to 120 nm. Because such micrographs correspond to very small sampling sizes, it was desirable, for quantitative purposes, to obtain more representative data. Direct measurement from a series of micrographs is always a tedious and subjective task. Light diffraction analysis of the negatives was considered as an alternative but spurious periodicities are known to result from strongly defocused images[28]. For these reasons, small angle electron diffraction was preferred; a 40 μm diameter region of the film could be averaged in one single measurement. The corresponding small angle diffraction patterns are shown in *Figure 11* (inserts), with proper orientation. They are characterized by a pair of maxima corresponding to the 'lamellar structure' and a streak originating from the fibrils. The intensity maxima clearly shift to higher angle for lower molecular weights.

DISCUSSION

Film structure

Earlier literature data[6,12,22] was generally derived from films obtained from sensibly less concentrated solutions and correspondingly longer crystallization times. Nevertheless, the general coagulation behaviour emerging from these previous investigations agrees well with the present findings. Data concerning the optical texture deserves little additional discussion, considering the vast amount of information published on this topic. The observed textures are not only similar to those previously described for PPTA, but also to those reported for many other lyo- or thermotropic systems[23,29]. In fact, early observation of such ordered textures date, at least, as far back as 1934 for a variety of systems involving shear- or flow-oriented solutions of suspensions of rigid molecules or molecular assemblies[30]. Fincher[31] recently confirmed, with lyotropic solutions of ethylcellulose, the earlier observations of Kulitchikhin *et al.*[32] on poly(*p*-benzamide) and of Horio *et al.*[5] on hydroxypropyl cellulose and PPTA showing that the banding does not arise during flow but immediately at the cessation of flow. In contradiction with the present data and literature data[7,22], Fincher also observed that the banding periodicity does not depend on the shear rate or the film thickness. In the present work, these parameters varied over a wider range.

The most spectacular feature observed at higher resolution in the sheared films is the row-nucleated morphology, originally described by Takahashi *et al.*[6]. Iovleva and Papkov[12], noticing the same fine structure in coagulated nematic solutions of poly(*p*-benzamide), revealed the existence of intermediate crystallosolvate structures. Our experimental set-up allowing separation of thermal and coagulation effects has resulted in supplementary information. Row-nucleated morphologies are obtained as a result of 'quench-only' conditions, i.e. formation of the crystallosolvate is required, and the morphology is best defined at low quench rates. At higher quench rates, embryonic row nucleated structures only are formed, reduced to quasi-fibrillar textures for the highest rates. A comparison with the poly(*p*-benzobisthiazole)/methane sulphonic acid system is here pertinent. The compared morphologies for slow and fast coagulation of this system have been recently described by Cohen *et al.*[33]. These authors have associated the fibrillar morphology to a direct transition to the solid polymer phase, and the lamellar morphology to the growth of an intermediate crystallosolvate phase. Such a distinction was not clearly possible in the present case because rather fibrillar morphologies were also obtained in 'quench only' experiments. These fibrillar structures may, however, slightly differ from the ones obtained by direct coagulation.

The influence of molecular weight on the morphology has been documented in the case of the row-nucleated structures. Takahashi *et al.*[6] speculated that the lamellar thickness was determined by the length of hydrolysed polymer chains. The present results indicate that a correspondence with the long period is more appropriate. This is dramatically illustrated in *Figure 12a* which presents equatorial traces for some typical patterns. In a crude analysis, justified because the actual morphology is known, one may calculate a long period from application of the Bragg law to the spacing for the maximum of the profile. After translation of the inherent viscosity values into chain lengths (using the relationship given in the experimental section), the long period may be plotted directly as a function of chain length as shown in *Figure 12b*. A direct relationship between chain length and long period is suggested. A more detailed description of molecular weight effects cannot be achieved because of the large polydispersity of such polymers (about 2) and the tremendous viscosity changes associated with molecular weight reduction. These results suggest a structure consisting of extended polymer chains bridging across the interlamellar space, with possibly a concen-

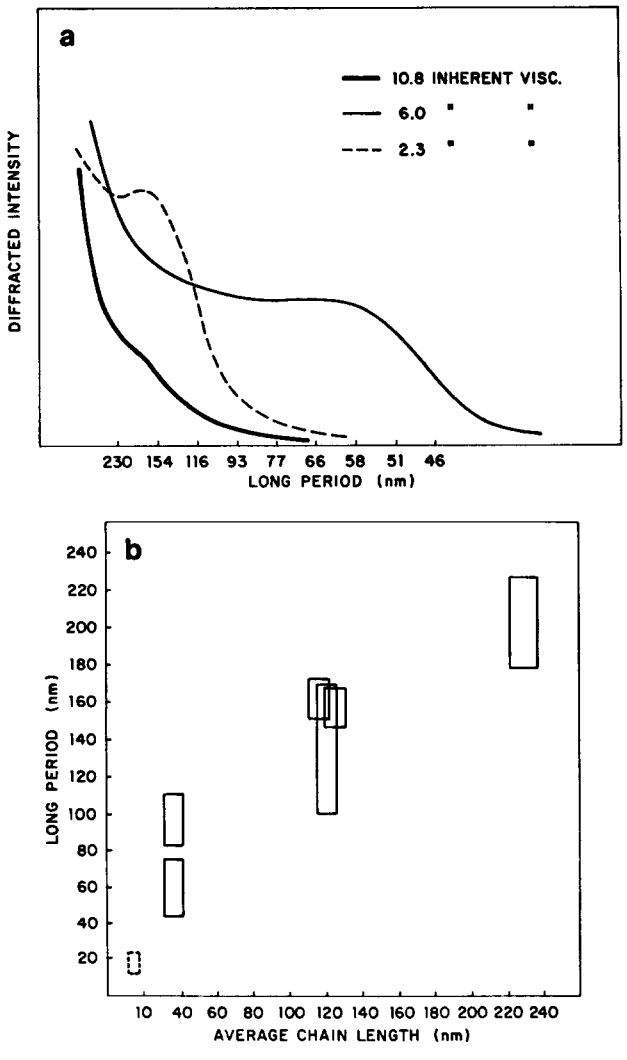

Figure 12 (a) Typical equatorial densitometer traces of small angle electron diffraction patterns like those shown in *Figure 11*. (b) Plot of the long period against the average chain length. The size of the boxes expresses the estimated experimental error

tration of chain ends at the interface. It is likely that molecular weight reduction, whether directly or through its accompanying increased chain mobility, favours such a concentration, therefore contributing to the more contrasted morphology in this case.

Finally, although the term 'lamella' has been loosely used to describe the row-nucleated morphology, its actual nature is questionable. Most striking is the darkfield image in *Figure 6* showing that the average crystalline shape remains characteristic of a fibrillar morphology. The abundance of interlamellar bridges is also notable, especially for the higher molecular weight polymers. There also exists a continuous gradation in the observed morphologies from 'lamellar' to fibrous. This is atypical of the conventional lamellar crystallization of flexible polymers. Such observations, and others on the PBZT system[34], suggest that the morphology may rather result from a cooperative twisting of ribbon-shaped fibrils. This fundamental crystallization behaviour of rigid rod systems should deserve further attention.

PPTA crystalline polymorphism

Electron diffraction data for the water coagulation experiments indicate that PPTA II may only be obtained as a result of the collapse of the solvated structure via water washing. More precisely, the following transformation scheme is proposed:

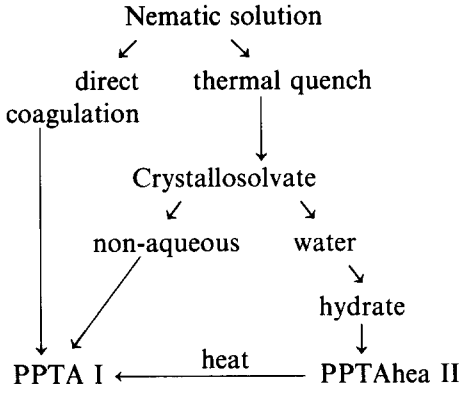

The scheme incorporates the intermediate hydrated structure proposed by Xu *et al.*[14]. It must be noticed that this scheme does not apply to low molecular weight PPTA; for this polymer, the more thermodynamically stable polymorph (PPTA I) was always obtained after water washing.

Remarkably, the crystalline polymorphism bears little relationship to the micromorphology because both polymorphs may be obtained in either fibrillar or row-nucleated morphology. This suggests that the row-nucleated structures are formed in the solvated state. The peculiarity of polymer crystallosolvates to maintain their gross morphology while undergoing total structural collapse has already been pointed out[12]. Such a behaviour may originate at the molecular level.

PPTA fibres

Finally, the question of the relevance of the above observations to the understanding of fibre structure formation and fibre properties must be addressed. The mechanism for pleat formation now appears clear. As the fluid spin dope enters the coagulation bath, a thin skin immediately forms which may support the threadline stresses. The rest of the liquid crystalline solution then relaxes, just as in the film shearing experiments (the skin playing the role of the glass slide). Also, similar to the film situation, the pleat pattern is not modified by subsequent coagulation. Such a mechanism was alluded to by Horio *et al.*[5] who showed that the banding (pleating) periodicity could be controlled by the coagulation speed. The authors have already accounted for modulus data in terms of the pleated structure: the steady modulus increase accompanying tensile stress (beyond inelastic deformation) corresponds to a reversible opening of the pleats[35,36].

The new advances in the understanding of PPTA polymorphism allow resolution of the apparent contradiction between Haraguchi's and Northolt's findings[9,10]. Although films and fibres are both coagulated in aqueous media, the two processes differ by their time scale, with enough time in the film experiments for a crystallosolvate to form. This scheme also provides a rationale for the presence of PPTA II in fibres coagulated at low temperature: slower diffusion of the coagulant leaves time for the solvated structure to crystallize[37]. For the inverse reason, it is unlikely that the crystallosolvate forms during regular spinning, contrary to the suggestion of

Gonio *et al.*[38]. Those authors based their analysis on the phase diagram for a system at equilibrium[13], which cannot be transposed to conditions where tremendous supercooling is likely.

More difficult is the question of fibre strength. Recent estimations of attainable strength for PPTA yielded values about twice the current Kevlar® strength of about 3.4 GPa, for a similar molecular weight and molecular weight distribution[39]. An ideally staggered chain end distribution was assumed, but even a slight degree of end clustering would have drastic consequences on the achievable strength[40]. Row-nucleated structures were never encountered in the experiments designed to mimic the fibre process, i.e. where thin films were directly coagulated in water. This was particularly the case for experiments with shear rates as high as $10^{5\circ}\,s^{-1}$, i.e. rather close to those experienced in spinning. This is counterbalanced by indirect evidence, mostly from the work of Panar *et al.*[41], for periodic defects. Fibre etching experiments revealed a system of defect lines perpendicular to the fibre axis and spaced about 30 nm apart. They were interpreted as resulting from the preferential etching of chain-end-rich regions. A similar experiment has since been repeated on films, with identical results[22]. Although experiments of this type must be interpreted with great care as being prone to artefact[42], soft X-ray small angle data did suggest existence of a similar periodicity in intact fibres[43]. Such a clustering has also been suggested from a detailed analysis of aramid fibre X-ray data[44]. Morgan *et al.*[45] proposed a model of structure based upon such ideas. The model, however, associated 'pleat' periodicity and chain end clustering on the basis of an erroneous estimate of the polymer molecular weight.

ACKNOWLEDGEMENTS

The authors are particularly grateful to their colleagues Y. Termonia and K. Gardner for their interest and suggestions in the course of this work and to Professor P. Smith for stimulating discussions. The technical assistance of J. Freida and C. Osier is acknowledged.

REFERENCES

1 Blades, H. US Patent 3 869 429, 1973
2 Schaefgen, J. R. in 'The Strength and Stiffness of Polymers' (Eds. A. E. Zachariades and R. S. Porter), Dekker, New York, 1983, p. 327
3 Ballou, J. W. *Polym. Prepr., ACS Polym. Chem. Div.* 1976, **17**, 75
4 Dobb, M. G., Johnson, D. J. and Saville, B. P. *J. Polym. Sci., Phys.* 1977, **15**, 2201
5 Horio, M., Ishikawa, S. and Oda, K. *J. Appl. Polym. Sci., Appl. Polym. Symp.* 1985, **41**, 269
6 Takahashi, T., Iwamoto, H., Inoue, K. and Tsujimoto, I. *J. Polym. Sci., Phys.* 1979, **17**, 115
7 Xu, D., Okuyama, K., Kumamaru, F., Takayanagi, M., Zhang, S. and Qian, R. *J. Polym. Sci., Polym. Lett.* 1982, **20**, 159
8 Takahashi, T., Susuki, S. and Tsujimoto, I. *Kobunshi Ronbunshu* 1977, **34**, 29
9 Northolt, M. G. *European Polym. J.* 1974, **10**, 799
10 Haraguchi, K., Kajiyama, T. and Takayanagi, M. *J. Appl. Polym. Sci.* 1979, **23**, 915
11 Arpin, M., Strazielle, C. and Skoulios, A. *J. Phys.* 1977, **38**, 307
12 Iovleva, M. M. and Papkov, S. P. *Vysokomol. Soyed.* 1982, **A24**, 233
13 Gardner, K. H., Matheson, R. R., Avakian, P., Chia, Y. T. and Gierke, T. D. *Polym. Prepr., ACS Polym. Chem. Div.* 1983, **24**(2), 469
14 Xu, D., Okuyama, K., Kumamaru, F. and Takayanagi, M. *Polym. J.* 1984, **16**, 31
15 Ryan, R. P., Purse, D. H., Robinson, S. G. and Wood, J. W. *J. Microsc.* 1987, **145**, 89
16 Yau, W. W., private communication
17 Baird, D. G., Smith, J. K. *J. Polym. Sci., Chem.* 1978, **16**, 61
18 Arpin, M. and Strazielle, C. *Polymer* 1977, **18**, 591
19 Ying, Q., Chu, B., Qian, R., Bao, J., Zhang, J. and Xu, C. *Polymer* 1985, **26**, 1401
20 Schaefgen, J. R., Foldi, V. S., Logullo, F. M., Good, V. H., Gulrich, L. W. and Killian, F. L. *Polym. Prepr., ACS Polym. Chem. Div.* 1976, **17**, 69
21 Ogata, N., Sanui, K. and Kitayanaga, S. *J. Polym. Sci., Chem.* 1984, **22**, 865
22 Chen, S., Jin, Y. and Qian, R. *Makromol. Chem.* 1987, **188**, 2713
23 Donald, A. M. and Windle, A. H. *J. Mat. Sci.* 1983, **18**, 1143
24 Roche, E. J., Wolfe, M. S., Suna, A. and Avakian, P. *J. Macromol. Sci., Phys.* 1985–1986, **B24**, 141
25 Gohil, R. M. and Peterman, J. *J. Polym. Sci., Phys.* 1979, **17**, 525
26 Haraguchi, K., Kajiyama, t. and Takayanagi, M. *J. Appl. Polym. Sci.* 1979, **23**, 902
27 Shen, D. Y., Molis, S. E. and Hsu, S. L. *Polym. Eng. Sci.* 1983, **23**, 543
28 Roche, E. J. and Thomas, E. L. *Polymer* 1981, **22**, 333
29 Nishio, Y. and Takahashi, T. *J. Macromol. Sci., Phys.* 1984–1985, **B23**, 483
30 Van Iterson, G. *Proc. Akad. Wetensch. Amsterdam* 1934, **37**, 367
31 Fincher, C. personal communication
32 Kulichikhin, V. G., Vasil'yeva, N. V., Platonov, V. A., Malkin, A. Ya., Belousova, T. A., Khanchich, O. A. and Papkov, S. P. *Vysokomol. Soyed.* 1979, **A21**, 1407
33 Cohen, Y. and Thomas, E. L. *ACS Symp. Ser.* 1987, **350**, 181
34 Roche, E. J. unpublished data
35 Roche, E. J., Allen, S. R., Fincher, C. R. and Paulson, C. *Liq. Cryst. Mol. Cryst.* 1987, **153**, 547
36 Allen, S. R. and Roche, E. J. *Polymer* 1989, **30**, 996
37 Fujiwara, T. and Ishitobi, T. Japan Patent Application, 59-1710, 1984
38 Gonio, G., Bruzzone, R., Ciferri, A., Bianchi, E. and Tealdi, A. *Polym. J.* 1987, **19**, 757
39 Termonia, Y. and Smith, P. *Polymer* 1986, **27**, 1845
40 Termonia, Y. private communication
41 Panar, M., Avakian, P., Blume, R. C., Gardner, K. H., Gierke, T. D. and Yang, H. H. *J. Polym. Sci., Phys.* 1983, **21**, 1955
42 Herms, J., Peebles, L. H. and Uhlmann, D. R. *J. Mat. Sci.* 1983, **18**, 2517
43 Herglotz, H. K. *J. Colloid Interface Sci.* 1980, **75**, 105
44 Krenzer, E. and Ruland, W. *Colloid and Polym. Sci.* 1985, **263**, 554
45 Morgan, R. J., Pruneda, C. O. and Steele, W. J. *J. Polym. Sci., Phys.* 1983, **21**, 1757